

Metal Nanoparticles with Gain toward Single-Molecule Detection by Surface-Enhanced Raman Scattering

Zhi-Yuan Li*

Laboratory of Optical Physics, Beijing National Laboratory for Condensed Matter Physics, Institute of Physics, Chinese Academy of Sciences, P.O. Box 603, Beijing 100190, China

Younan Xia

Department of Biomedical Engineering, Washington University, St. Louis, Missouri 63130

ABSTRACT Single-molecule detection via surface-enhanced Raman scattering (SERS) has raised great interest over the past decade. The usual approach toward this goal is to harness the strong surface plasmon resonance of light with complex metallic nanostructures, such as particle aggregates, two-particle gaps, sharp tips, or particles with sharp apexes. Here we propose another route toward the goal by introducing gain medium into single metal nanoparticles with simple geometry. Our calculations show that cubic gold nanobox particles that contain a gain material within the core can create an extremely high enhancement factor of local field intensity larger than 10^8 and a SERS enhancement factor on the order of 10^{16} – 10^{17} .

KEYWORDS Metal nanoparticles, gain, surface plasmon resonance, local field enhancement, SERS

Single-molecule detection via surface-enhanced Raman scattering (SERS) has been a subject of extensive research in the past decades due to its great impact in a wide variety of scientific and technological areas.^{1,2} A common approach to achieving this goal is to attach the molecules to metal nanoparticles and detect their enhanced Raman signals. When light interacts with metal nanoparticles, it will induce strong oscillation of conduction electrons known as surface plasmon resonance (SPR), leading to orders of magnitude enhancement for the local electric field intensity and Raman scattering signals at the surface of the metal nanoparticles. Several schemes have been explored to achieve single-molecule sensitivity. Complex metal nanoparticle aggregates can generate “hot spots” where the SERS enhancement factor (*G* factor) can be as high as 10^{14} – 10^{15} , a level that is sufficient for single-molecule detection.^{3,4} Another scheme is to utilize dimers of metal nanoparticle where the two particles almost touch, together with a tiny gap on the scale of several nanometers to generate a *G* factor of 10^{11} – 10^{12} .^{5–8} A similar scheme is to use a sharp metallic tip to create strongly enhanced local field at its vicinity.^{9–11} Active control over SERS can be realized by adjusting the tip–substrate distance. The above schemes involve complicated morphology of metallic particles, and the volume ratio

of the “hot spot” regions over the whole system is low, leading to limited efficiency for SERS detection.

To overcome these problems, single metal nanoparticles with simple geometry are highly desired, provided that they can offer sufficiently high *G* factors. It has been well-established that large local-field enhancement is closely related to metal nanostructures with sharp corners or small curvatures because electric charges tend to accumulate in these regions and result in high electric field intensity. Single nanoparticles with sharp corners, such as cubes or rectangular bars¹² and nanoprisms,^{13,14} have been shown to exhibit very strong local field enhancement. Nonetheless, the local-field amplitude enhancement factor for these structures with sharp corners is limited to a level that is well below several hundreds. In general, it is very hard to use these nanoparticles to obtain a *G* factor well beyond 10^{11} – 10^{12} .

Recently it was proposed that introduction of a gain material into metal nanoparticles or nanostructures can lead to surface plasmon amplification of stimulated emission of radiation (spacer).¹⁵ The physical essence is the plasmon-resonance-mediated light amplification of radiation from the gain material. Later on, light amplification through plasmonic structures containing gain materials was demonstrated theoretically¹⁶ and experimentally.^{17,18} Theoretical study on core–shell concentric spherical nanoparticles made from an inner gained dielectric core coated with an outer metal thin film shows that amplification of light by the gain medium can be enhanced by several orders of magnitude through SPR.¹⁹ All these studies clearly illustrate promising

* To whom correspondence should be addressed. lizy@aphy.iphy.ac.cn.

Received for review: 10/12/2009

Published on Web: 12/03/2009

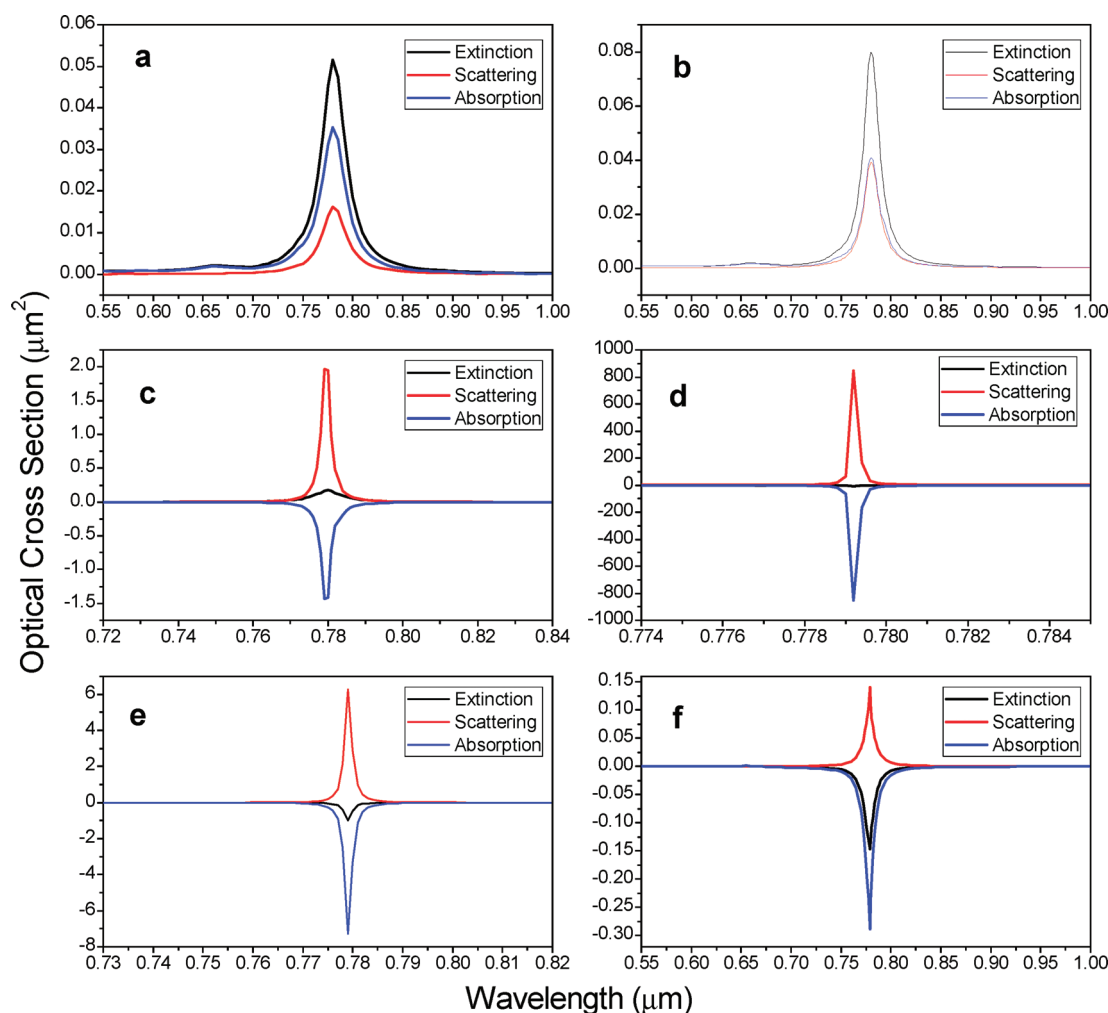


FIGURE 1. Calculated optical cross section spectra for a cubic Au nanobox containing gain materials with different gain coefficients κ_{core} in the core. The nanobox is immersed in water. Panels a–f correspond to κ_{core} values of 0, 0.05, 0.13, 0.143, 0.15, and 0.2, respectively. Resonance coupling between incident light and the local SPP modes takes place at about 779 nm, where significant enhancement of optical cross section is observed. Note that a negative absorption cross section means amplification of light when it passes through the nanobox. Over 4 orders of magnitude enhancement of scattering and amplification by the metallic particle are observed when the core gain coefficient reaches a value of 0.143. At the same time, the line width of the optical spectrum is drastically reduced to about 0.3 nm.

aspects and appealing power of light amplification by combining SPR with an ordinary gain medium in a nanosystem.

In this paper we show that these active metal nanosystems also provide intriguing power to enhance local electric field intensity to a high level where single-molecule detection by SERS can be readily achieved. We have made a systematic analysis on the local field enhancement characteristic of cubic gold nanobox that contains gain material within the core. Our numerical simulations show that the composite metal nanoparticle can generate an extremely high enhancement factor of local field intensity exceeding 10^8 and a G factor on the order of 10^{16} – 10^{17} .

Results and Discussion. The active nanosystem we consider here is a cubic Au nanobox with a gain material encapsulated in the core. The outer and inner edge lengths of the Au nanobox are 40 and 32 nm, respectively, with the thickness of all six walls being 4 nm. Such nanostructures can be easily synthesized using the galvanic replace-

ment reaction between single-crystal Ag nanocubes and HAuCl_4 .^{20,21} The SPR peaks of these nanoboxes can be conveniently tuned from the visible to the near-infrared region, in particular with strong absorption at a wavelength around 800 nm for biomedical applications such as early cancer diagnosis and photothermal treatment.^{20,21}

Figure 1a shows the calculated optical spectra of extinction (C_{ext}), scattering (C_{sca}), and absorption (C_{abs}) cross sections for the Au nanobox by means of the discrete-dipole approximation (DDA) method.^{22,23} Here the nanobox is immersed in water with a refractive index of 1.33, and the core region is also filled with water. The incident light propagates parallel to the [001] direction of the cubic particle, and the electric field with an amplitude E_0 is polarized parallel to the [100] direction. A sharp SPR peak is centered at about 779 nm, where the total extinction cross section is about $0.05 \mu\text{m}^2$, nearly 30 times the geometrical cross section of the particle. The line width (Δ_{SPR}) of the peak

is about 50 nm, and the low quality factor of plasmonic resonance can be mainly attributed to the strong dissipation of conduction electrons in Au. In addition, C_{abs} is about twice that of C_{sca} , indicating a strong absorption characteristic for the particle. The calculated local electric field distribution pattern (the data will be shown below) indicates that at resonance, the maximum local field amplitude is slightly below 100 times the incident field amplitude, not a very large enhancement factor.

The picture is drastically different when a gain material is introduced into the core region. A model system is considered where a gain coefficient κ_{core} is introduced into the core medium to describe phenomenologically the response of the incident light to the gain material. In particular, we simply set a complex refractive index of $n - i\kappa_{\text{core}}$ for the medium in the core region, where n is fixed at 1.33 and κ_{core} can vary depending on the extent of amplification.

Parts b–f of Figure 1 illustrate the calculated optical cross section spectra for different values of κ_{core} . One interesting feature is that the SPR peak remains at the same wavelength of about 779 nm. Another interesting feature is that the quantity and line shape of the optical spectra strongly depend on the gain coefficient. For κ_{core} as small as 0.05, the spectrum is similar to the case of a passive Au nanobox, albeit there is an increase for the quantity of C_{ext} and C_{sca} , together with a 2-fold reduction for Δ_{SPR} to about 25 nm. When κ_{core} increases to a value of 0.13, C_{sca} becomes greatly enhanced, by almost 50 times. The absorption of light by metal is also remarkably increased, but is now compensated by the amplification from the gain material, leading to negative absorption (i.e., amplification) of light by the composite, active nanoparticle. C_{ext} also increases, but in a much smaller magnitude, due to a compromise between the scattering loss and amplification gain. Δ_{SPR} of the SPR peak greatly decreases to about 5 nm. When κ_{core} further increases to a critical value, which is about 0.143 for the current nanosystem, a significant resonance takes place, as shown in Figure 1d. Δ_{SPR} drastically drops to a small value of below 0.3 nm. The scattering cross section is $845 \mu\text{m}^2$, or 16000 times the value of the passive Au nanobox, and the overall amplification cross section is also greatly enhanced to $854 \mu\text{m}^2$, which is 50000 times the value of the passive counterpart (Figure 1a). The overall extinction cross section is a negative value, which means that the nanosystem can amplify the incident light although scattering along all directions is so strong. All these features clearly indicate the initiation of lasing.

When the gain coefficient continues to grow and slightly exceeds the critical value, i.e., $\kappa_{\text{core}} = 0.15$, the nanosystem is rapidly off resonance, with Δ_{SPR} increasing to about 3 nm. However, the scattering and amplification by the nanosystem are still more than 2 orders of magnitude larger than in the passive Au nanobox. When κ_{core} further increases to a value of 0.20, the enhancement of the light–nanosystem interaction is no longer in place. Unlike the situation of a

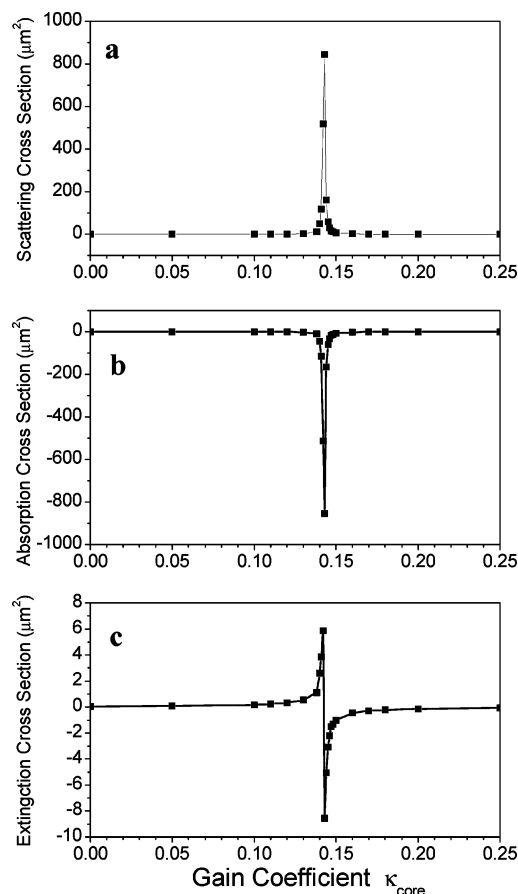


FIGURE 2. Resonant optical scattering (a), absorption (b), and extinction (c) cross sections for a cubic Au nanobox as a function of the gain coefficient κ_{core} of a gain material in the core with an excitation wavelength of 779.2 nm. Maximum light–particle interaction takes place at $\kappa_{\text{core}} = 0.143$, where the scattering cross section is over 2×10^4 times the value for a Au nanobox containing no gain material and the amplified cross section is 4×10^6 times the value for a cubic nanoparticle of the pure gain material with the same size. The extinction spectrum shows a sharp crossover from strong attenuation to strong amplification around the resonance.

small gain coefficient, the amplification of light in the nanosystem dominates over the scattering of light with $-C_{\text{abs}}/C_{\text{sca}} \approx 2$, leading to a net gain of light.

Figure 2 illustrates the calculated peak quantity of scattering, absorption, and extinction cross section at the resonance wavelength of 779.2 nm as a function of κ_{core} of the gain material. The sharp resonance at the critical point of κ_{core} can be clearly seen, at which the full width at half-maximum for the resonance peak is below 0.03. Within this narrow window both the scattering and absorption quickly jump to the peak value and then drastically drop, while the extinction drops from a large positive value at $\kappa_{\text{core}} = 0.142$ to a large negative value at $\kappa_{\text{core}} = 0.143$, a behavior very similar to the familiar phase transition in condensed matter. These features, together with the sharp narrowing of the SPR peak, clearly indicate the induction of lasing at the critical point.

The derivative line shape of the extinction curve can be understood from a simple physical picture about the change

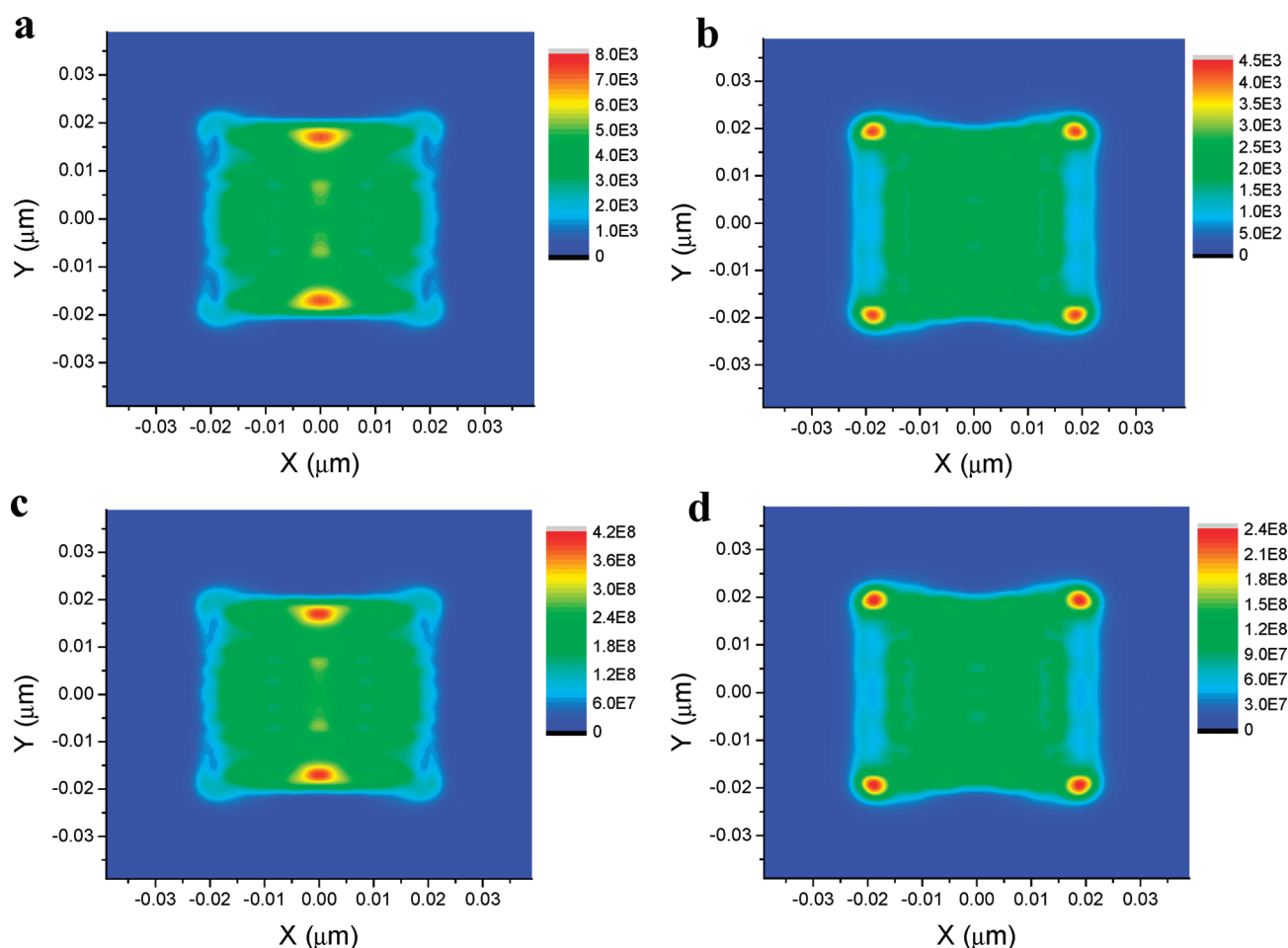


FIGURE 3. Calculated patterns of local electric field intensity for a cubic Au nanobox without (panels a and b) and with (panels c and d) a gain material. The nanobox is immersed in water. The gain material has a complex refractive index of $1.33 - 0.143i$. Panels a and c are at the XY plane that crosses the center of the wall and where the maximum local-field intensity spot is located, while panels b and d are at the front surface of the nanobox. The excitation wavelength is 779.2 nm.

of scattering by the nanoparticle, absorption by the metal medium, and amplification by the gain medium at different gain coefficients. At a small gain coefficient, the amplification of SPR due to gain medium will further enhance the absorption by the metal and scattering by the nanoparticle. As a result, the extinction coefficient remains a negative number and its absolute value keeps growing when the gain coefficient increases. When the gain coefficient is sufficiently large, the amplification of light will overwhelm the dissipation due to absorption by the metal medium and scattering by the nanoparticle. As a result, the extinction coefficient will become a negative number. There must be a transition between these two situations where the extinction coefficient changes its sign, and this takes place right at the resonance. The nanoparticle is turned from very dissipative to strongly amplifying when it transverse across this resonance point. This is exactly what we observe in Figure 2c.

To see the physical mechanism behind the observed lasing phenomenon, and whether it is induced by surface plasmon as in the concept of spacer, we take a close look at the local-field distribution pattern. Parts a and b of Figure 3

show the electric field intensity pattern in two XY planes perpendicular to the incident light propagation direction for a passive Au nanobox at the resonant wavelength of 779.2 nm. Panel a passes the middle of the front wall of the cubic nanobox. The calculation shows that the maximum local field spot is located at this plane with an intensity enhancement factor of about 8000. More precisely the two maximum-field spots are close to the upper and lower side edges of the cubic nanobox, instead of locating at the corner region. Figure 3b shows the electric field intensity pattern right at the front surface of the cubic Au nanobox, which is more relevant for the purpose of SERS detection. There are four high-field spots located near the apexes of the particle, with an intensity enhancement factor of 4500. The field is rather dispersed around on the entire surface, with an average intensity about one-half the value at the high-field spots.

The calculated field pattern for an active nanosystem with $\kappa_{\text{core}} = 0.143$ is illustrated in Figure 3, panels c and d, for the two XY planes, the same as in Figure 3, panels a and b, at the resonant wavelength of 779.2 nm. Two significant features are worth emphasizing. The first is the close similar-

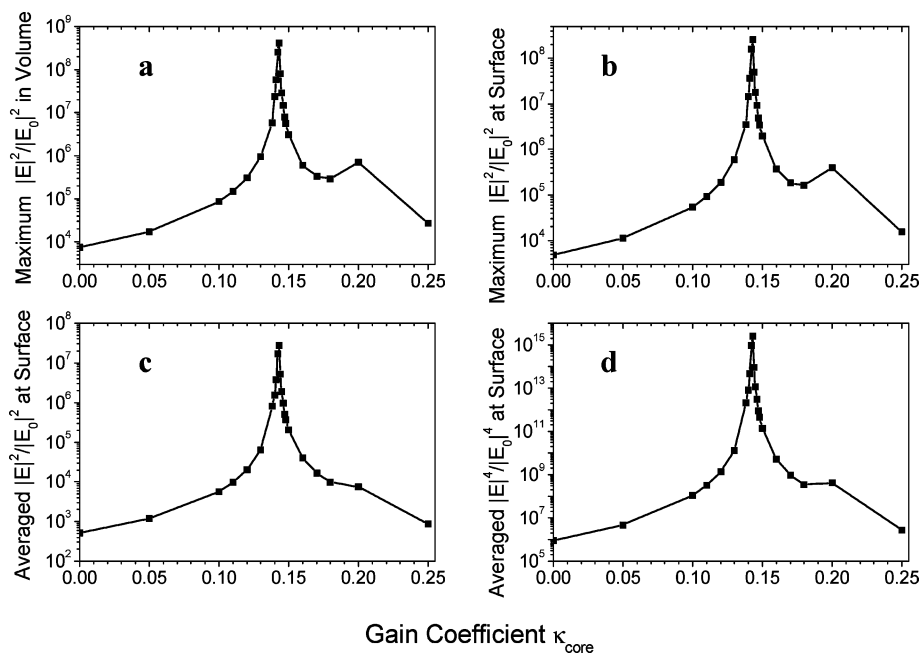


FIGURE 4. Maximum local-field intensity enhancement factor within the whole volume (a) and at the surface of the active metal nanobox particle (b), and enhancement factor for averaged field intensity (c) and SERS signal at the surface of the particle (d) as a function of the gain coefficient κ_{core} at a resonance wavelength of 779.2 nm.

ity of the field patterns between the active nanosystem and the passive counterpart. The field profile, as well as the number and location of the high-field spots, are almost identical to each other. The second and more interesting feature is the huge enhancement of local field intensity. The maximum field intensity enhancement factor is at an extremely high level of 4.2×10^8 , with the corresponding G factor at a level of 10^{17} . The average field intensity at the front surface is still at a high level of 1.0×10^8 , whereas the field intensity at the four hot spots can reach 2.4×10^8 . This means that the G factor over the entire front surface area of the active nanosystem can be as high as 1.0×10^{16} , a level that has not been reached by other types of metal nanoparticles.

A picture about such a huge field enhancement can now be constructed. The gain material in the core region of a Au nanobox does not change the basic properties of the surface plasmon polariton (SPP) mode that is excited by the incident light as the gain coefficient 0.143 is small compared to the complex refractive index of gold, $0.175 + 4.90i$ at 779 nm. However, the gain material will absorb energy from external pump source. By interacting with the SPP modes whose energy is dispersed all within and around the metal nanoparticle, the energy can transfer to SPP mode, causing its amplitude to grow. At the same time, at a critical value of gain coefficient, the nanosystem will achieve a balance between its loss due to absorption and scattering by the metal and amplification by the gain material. The relatively large Δ_{SPR} in a passive nanoparticle due to absorption dissipation is greatly reduced as the overall dissipation now disappears. This means that the quality factor of the plas-

monic nanosystem is significantly enhanced. As a result, the active nanosystem behaves like a high-quality nanoscale SPP cavity, where the ordinary accumulation effect can drastically increase the plasmonic energy density and electromagnetic field intensity. To some extent, the lasing of SPP or spacer has been realized in the current active nanosystem. It should be noticed that the current SPP lasing occurs only at a critical point of gain coefficient and below and above this threshold lasing disappears. This is very different from the traditional laser, where above the threshold lasing continues to act, albeit there is saturation in power for the output light. The reason is that the current active nanosystem is a strong coupling system between light, atom states, and SPP modes, and the output power is extremely sensitive to the gain coefficient as well as other physical parameters of the nanosystem.

Panels a and b of Figure 4 illustrate the maximum field intensity enhancement factor as a function of the gain coefficient when one looks at everywhere within and around the nanosystem (i.e., volume maximum) and when one only looks at the outer surface areas of the nanoparticle (i.e., surface maximum), respectively. Panels c and d of Figure 4 show the corresponding average intensity enhancement factor and G factor on the outer surface areas of the active nanosystem, respectively. The nanosystem is excited at a resonant wavelength of 779.2 nm. The calculation shows that the volume maximum is located near the edge of the nanobox particle, while the surface maximum is located near the corner of the particle. The volume maximum is about twice the surface maximum in quantity. There is a narrow window of κ_{core} around the critical point where the

surface maximum exceeds 1.0×10^7 , which extends from 0.140 to 0.146. At these surface “hot spots”, the SERS enhancement factor can exceed 1.0×10^{14} , a level where single-molecule detection should be possible. The window has a bandwidth of about $\Delta\kappa_{\text{core}} = 0.006$ and a normalized bandwidth of $\Delta\kappa_{\text{core}}/\kappa_{\text{core}} = 4\%$. So there is a promising tolerance for the active nanosystem to observe single molecule SERS signal with a single nanoparticle.

In practical single-molecule detection, it is difficult to only locate a single molecule in the “hot spot” region. It is then more interesting to see if the overall SERS G factor on the entire surface area of a metal nanoparticle can reach a sufficiently high level. Figure 4d shows that in the narrow window of κ_{core} from 0.140 to 0.145 the average surface G factor exceeds 1.0×10^{13} . Although the average G factor is 1 order of magnitude lower than in the surface “hot spots”, the surface area is at least 2 orders of magnitude larger than the area of these “hot spots”. So the overall possibility to observe a single molecule Raman signal is much higher when one utilizes the entire surface rather than only the “hot spot” region. In this regard, the current active nanosystem is very promising for realizing single-molecule detection in a single nanoparticle. At the critical point of $\kappa_{\text{core}} = 0.143$, the average surface field intensity enhancement factor is about 2.8×10^7 while the average G factor is at a very high level of 2.5×10^{15} . This means that at this condition the active nanosystem has a very promising potential for single-molecule detection by SERS.

Further Discussion. A gain coefficient on the order of $\kappa_{\text{core}} = 0.143$ corresponds to an amplification coefficient of light intensity as $g = 4\pi\kappa_{\text{core}}/\lambda$, which is $2.31 \times 10^4/\text{cm}$ for a wavelength of 779 nm. This amplification coefficient is modest and accessible in practice. The gain material can be made either from dye molecules,¹⁸ semiconductor nanoparticles with sizes of a few nanometers,²⁴ or from rare earth ions such as Er^{3+} .²⁵ In general, the gain coefficient is related to both the emission cross section σ_e and the concentration N in these gain systems, which can be written as $g = N\sigma_e$, and the corresponding gain coefficient is given by

$$\kappa_{\text{core}} = \frac{\lambda}{4\pi}g = \frac{\lambda}{4\pi}N\sigma_e$$

From this formula one can find that the key toward a sufficient large gain coefficient is to have a gain system with a large emission cross section and a high concentration.

In ref²⁶ T5oCx films were cast by spin coating a chloroform solution on glass slides, where the concentration of dye molecules was about $7.0 \times 10^{-2} \text{ M} = 4.22 \times 10^{19}/\text{cm}^3$ and the gain cross section is about $6.0 \times 10^{-16} \text{ cm}^2$ from pump–probe measurements at 610 nm. From this we can estimate the gain coefficient in this condition as $g = N\sigma_e = 2.532 \times 10^4/\text{cm}$ and

$$\kappa_{\text{core}} = \frac{\lambda}{4\pi}N\sigma_e = 0.123$$

For Er-fiber lasers in the infrared region, the typical concentration is on the order of $3 \times 10^{20}/\text{cm}^3$. The studies in refs²⁷

and²⁸ with Er-doped silicon nanocrystals have achieved a cross section on the order of 10^{-16} cm^2 , so that we can estimate the gain coefficient of Er-doped glass at the wavelength of 1550 nm as $g = N\sigma_e = 3.0 \times 10^4/\text{cm}$ and

$$\kappa_{\text{core}} = \frac{\lambda}{4\pi}N\sigma_e = 0.37$$

As to the quantum dot system, Kirstaedter et al. reported a large material gain of $g = 6.8 \times 10^4/\text{cm}$. This system can offer sufficiently strong gain coefficient for the metal nanoparticle with gain that we have discussed in the above for the sake of a giant field enhancement.

Although in the above discussions we have only considered Au nanoboxes with surface plasmon resonance occurring at about 780 nm, this resonance wavelength can be freely tuned by changing the geometric parameters of the nanobox, such as its edge length and the wall thickness. In this way, we can design and synthesize appropriate Au nanoboxes to match the excitation wavelength window for particular gain molecules, ions, or quantum dots. On the other hand, it is also possible to design other types of metal nanoparticles with appropriate geometry so that the required gain coefficient can be further reduced. In order to achieve sufficiently strong optical gain, an ordinary optical pumping by shorter wavelength light can be used. As the wall of the Au nanoparticle is only several nanometers thick, the pump light should be able to efficiently penetrate into the core region and excite the gain medium there.

Conclusions. We have investigated the local field enhancement characteristic of gold nanobox particles with a gain medium embedded within their core region and found that the composite active nanoparticles can create an extremely high enhancement factor of local field intensity that exceeds 10^8 and a SERS enhancement factor on the order of 10^{16} – 10^{17} , which is sufficient for single-molecule detection. The effect is attributed to the amplification of metal nanoparticle SPR by the gain medium under pumping of the incident light. The proposed scheme of a single Au cubic nanobox containing a gain material in the core region has several advantages. First, the SPR peak in these nanoboxes is readily adjustable from the visible to the near-infrared regions by controlling the edge length and wall thickness of the nanoboxes. This can be very useful for single-molecule SERS detection using different laser wavelengths. Second, the SPR in these nanoparticles is strong, which facilitates strong coupling among the SPP, active atom states, and light. The transfer of energy from the gain material will feed the SPP mode, amplify its amplitude and energy, and attain lasing of spacer at a critical point of gain coefficient. This in turn causes significant light scattering, absorption of light by the metal, and amplification of light by the gain material, all of which gigantically increase the local electromagnetic field intensity within and around the active nanosystem to a level far exceeding the single-molecule SERS detection limit. Third, the strong field not only concentrates on several “hot spots” but also spreads over the entire outer surface of

the nanoparticle, leading to a sufficiently high level of average field intensity and G factor enhancement. As the entire surface can be harnessed for single-molecule SERS detection, the efficiency of signal observation can be greatly improved. Finally, the Au nanoboxes can be synthesized in copious quantities by means of a simple chemical approach, have simple geometry, have sufficient mechanical stability, and are easy to operate on. The corners of the nanoboxes can also be truncated off to generate a nanocage to allow for loading of the gain material into the core region.²¹ These features will be beneficial to the demonstration of lasing and fabrication of practical device for single-molecule SERS detection.

Acknowledgment. The author (Z.Y.L.) would like to acknowledge financial support from the National Natural Science Foundation of China under Grants 10525419, 60736041, and 10874238 and the State Key Development Program for Basic Research of China under Grants 2006CB302901 and 2007CB613205.

REFERENCES AND NOTES

- (1) Moskovits, M. *Rev. Mod. Phys.* **1985**, *57*, 783–826.
- (2) Campion, A.; Kambhampati, P. *Chem. Soc. Rev.* **1998**, *27*, 241–250.
- (3) Kneipp, K.; Wang, Y.; Kneipp, H.; Perelman, L. T.; Itzkan, I.; Dasari, R. R.; Feld, M. S. *Phys. Rev. Lett.* **1997**, *78*, 1667–1670.
- (4) Nie, S.; Emory, S. R. *Science* **1997**, *275*, 1102–1106.
- (5) Xu, H.; Bjerneld, E. J.; Käll, M.; Börjesson, L. *Phys. Rev. Lett.* **1999**, *83*, 4357–4360.
- (6) Xu, H.; Aizpurua, J.; Käll, M.; Apell, P. *Phys. Rev. E* **2000**, *62*, 4318–4324.
- (7) Lassiter, J. B.; Aizpurua, J.; Hernandez, L. I.; Brandl, D. W.; Romero, I.; Lal, S.; Hafner, J. H.; Nordlander, P.; Halas, N. J. *Nano Lett.* **2008**, *8*, 1212–1218.
- (8) Schuck, P. J.; Fromm, D. P.; Sundaramurthy, A.; Kino, G. S.; Moerner, W. E. *Phys. Rev. Lett.* **2005**, *94*, 017402.
- (9) Pettinger, B.; Ren, B.; Picard, G.; Schuster, R.; Ertl, G. *Phys. Rev. Lett.* **2004**, *92*, No. 096101.
- (10) Wang, X.; Liu, Z.; Zhuang, M. D.; Zhang, H. M.; Wang, X.; Xie, Z. X.; Wu, D. Y.; Ren, B.; Tian, Z. Q. *Appl. Phys. Lett.* **2007**, *91*, 101105.
- (11) Bortchagovsky, E.; Klein, S.; Fischer, U. C. *Appl. Phys. Lett.* **2009**, *94*, No. 063118.
- (12) McLellan, J. M.; Li, Z. Y.; Siekkinen, A. R.; Xia, Y. *Nano Lett.* **2007**, *7*, 1013–1017.
- (13) Kelly, K. L.; Coronado, E.; Zhao, L. L.; Schatz, G. C. *J. Phys. Chem. B* **2003**, *107*, 668–677.
- (14) Rang, M.; Jones, A. C.; Zhou, F.; Li, Z. Y.; Wiley, B. J.; Xia, Y.; Raschke, M. B. *Nano Lett.* **2008**, *8*, 3357–3363.
- (15) Bergman, D. J.; Stockman, M. I. *Phys. Rev. Lett.* **2004**, *90*, No. 027402.
- (16) Zheludev, N. I.; Prosvirnin, S. L.; Papasimakis, N.; Fedotov, V. A. *Nat. Photonics* **2008**, *2*, 351–354.
- (17) Plum, E.; Fedotov, V. A.; Kuo, P.; Tsai, D. P.; Zheludev, N. I. *Opt. Express* **2009**, *10*, 8548–8551.
- (18) Noginov, M. A.; Zhu, G.; Belgrave, A. M.; Bakker, R.; Shalae, V. M.; Narimanov, E. E.; Stout, S.; Herz, E.; Suteewong, T.; Wiesner, U. *Nature* **2009**, *460*, 1110–1113.
- (19) Gordon, J. A.; Ziolkowski, R. W. *Opt. Express* **2007**, *15*, 2622–2653.
- (20) Chen, J.; Saeki, F.; Wiley, B. J.; Cang, H.; Cobb, M. J.; Li, Z. Y.; Au, L.; Zhang, H.; Kimmey, M. B.; Li, X.; Xia, Y. *Nano Lett.* **2005**, *5*, 473–477.
- (21) Chen, J.; Wiley, B.; Li, Z. Y.; Campbell, D.; Saeki, F.; Cang, H.; Au, L.; Lee, J.; Li, X.; Xia, Y. *Adv. Mater.* **2005**, *17*, 2255–2261.
- (22) Goodman, J. J.; Draine, B. T. *Opt. Lett.* **1991**, *16*, 1198–1200.
- (23) Zhou, F.; Li, Z. Y.; Liu, Y.; Xia, Y. *J. Phys. Chem. C* **2008**, *112*, 20233–20240.
- (24) Carrere, H.; Marie, X.; Lombez, L.; Amand, T. *Appl. Phys. Lett.* **2006**, *89*, 181115.
- (25) Desurvire, E. *Erbium Doped-fiber Amplifiers*; John Wiley and Sons: New York, 1994.
- (26) Pisignano, D.; Anni, M.; Gigli, G.; Cingolani, R.; Zavelani-Rossi, M.; Lanzani, G.; Barbarella, G.; Favaretto, L. *Appl. Phys. Lett.* **2002**, *81*, 3534–3536.
- (27) Priolo, F.; Franco, G.; Pacirci, D.; Vinciguerra, V.; Fabio Iacona, F.; Irrera, A. J. *Appl. Phys.* **2001**, *89*, 264–272.
- (28) Kenyon, A. J.; Chryssou, C. E.; Pitt, C. W.; Shimizu-Iwayama, T.; Hole, D. E.; Sharma, N.; Humphreys, C. J. *J. Appl. Phys.* **2002**, *91*, 367–374.
- (29) Kirstaedter, N.; Schmidt, O. G.; Ledentsov, N. N.; Bimberg, D.; Ustinov, V. M.; Egorov, A. Yu.; Zhukov, A. E.; Maximov, M. V.; Kop'ev, P. S.; Alferov, Zh. I. *Appl. Phys. Lett.* **1996**, *69*, 1226–1228.